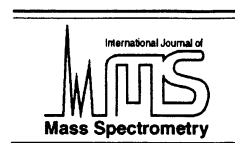




ELSEVIER

International Journal of Mass Spectrometry 195/196 (2000) 101–114



High-energy [C,H₃,N,O] cation radicals and molecules

Miroslav Polášek, Martin Sadílek, František Tureček*

Department of Chemistry, Bagley Hall, Box 351700, University of Washington, Seattle, WA 98195, USA

Received 11 May 1999; accepted 6 July 1999

Abstract

[C,H₃,N,O] cation radicals and molecules corresponding to the less stable isomers were investigated by a combination of ab initio and density functional calculations, and collision-induced dissociation and neutralization-reionization mass spectrometric measurements. The ions formed by loss of oxygen from a nitromethane cation radical and loss of hydroxyl radical from protonated nitromethane were identified as having the nitrosomethane structure (**2**⁺). A novel rearrangement in the ethyl nitrite cation radical was found to result in an elimination of formaldehyde to produce **2**⁺ but not isonitrosomethane, CH₃ON⁺ (**3**⁺). Dissociations of **2**⁺ and **2** were investigated by variable-time neutralization-reionization mass spectrometry. Cleavage of the C–N bond was found to occur in both the neutral and ion with comparable rate constants. Ab initio calculations provided C–N bond dissociation energies that were very similar in **2** and **2**⁺, 161 and 164 kJ mol⁻¹, respectively. The calculated heats of formation, adiabatic and vertical ionization energies, and recombination energies are reported for six [C,H₃,N,O] ion and neutral isomers, formamide, nitrosomethane, isonitrosomethane, formaldoxime, formaldonitrone, and oxaziridine. (Int J Mass Spectrom 195/196 (2000) 101–114) © 2000 Elsevier Science B.V.

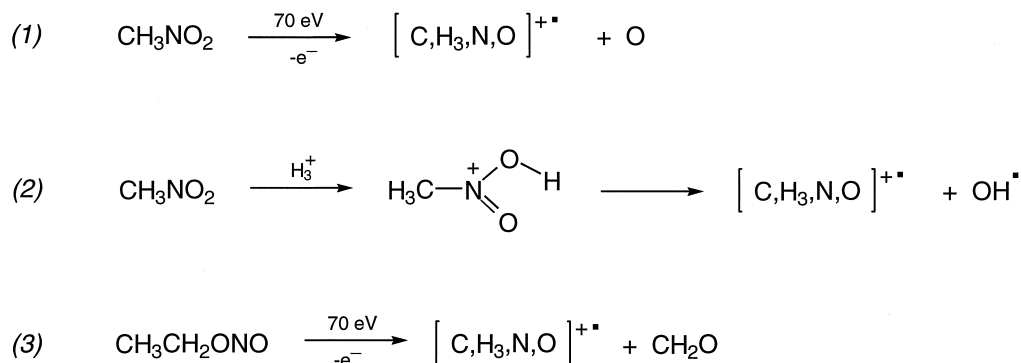
Keywords: Neutralization reionization; Variable-time measurements; Nitrosomethane; Isonitrosomethane

1. Introduction

Gas-phase cations containing N–O bonds in nitro, nitroso, and nitrite functional groups often undergo unimolecular rearrangements [1]. Migrations of hydrogen atoms [2–7], oxygen [8,9], alkyl [2,3,6,8–10], and aryl groups [11–13] have been observed and studied [14–16], as reviewed [17]. In the course of our studies of cationic precursors for nitro, nitroso, and nitrite radicals by neutralization-reionization mass spectrometry (NRMS) [18], we observed the formation of [C,H₃,N,O]⁺ cations due to three dis-

tinct dissociations shown in Scheme 1. The structures and relative energies of these cations were therefore of interest as were those of the corresponding neutral molecules. Out of the [C,H₃,N,O] family of isomers only formamide (**1**) is sufficiently stable in the condensed phase to allow thermochemical measurements. Nitrosomethane (**2**) is a reactive compound that undergoes spontaneous dimerization and tautomerization to formaldoxime (**4**) upon standing [19–21]. Isonitrosomethane (**3**) has not been prepared so far. Compounds **2** and **4**, generated as monomers in the gas phase [22–24], have been studied by a variety of spectroscopic methods [24–26] and ab initio calculations [27–32]. The gas-phase ion chemistry of [C,H₃,N,O]⁺ isomers has been studied in some detail by Hop et al. [33], who focused on the more stable

* Corresponding author. E-mail: turecek@chem.washington.edu
Dedicated to the memory of Robert R. Squires.



Scheme 1.

isomers of this group. However, the thermochemistry of the high-energy, less accessible $[\text{C},\text{H}_3,\text{N},\text{O}]$ isomers relied on estimates [33] and ab initio calculations for ions [23] and neutral molecules [23,27–32] that were performed at different levels of theory.

In this work we report on the formation and mass spectrometric characterization of nitrosomethane cation radical (2^+). Neutralization-reionization mass spectrometry [34] combined with variable-time measurements [35,36] are used to characterize neutral nitrosomethane (**2**). In order to compare the ion and neutral thermochemistry at a uniform level of theory, G2(MP2) ab initio calculations combined with density functional theory geometry optimizations are used to provide heats of formation, dissociation, ionization, and Franck–Condon energies for several $[\text{C},\text{H}_3,\text{N},\text{O}]$ cation radicals and neutral molecules containing N–O bonds.

2. Experimental

2.1. Methods

Measurements were performed on a homebuilt tandem quadrupole acceleration deceleration mass spectrometer that has been described in detail previously [37]. Typical conditions for electron ionization were as follows: Electron energy 70 eV, electron current 500 μA , ion energy 70 eV, and source temperature 270–300 °C. Chemical ionization was carried out in a tight ion source of our design using

$\text{CH}_5^+/\text{CH}_4$ or H_3^+/H_2 as reagents. The ions were extracted from the source and passed through a quadrupole operated in the rf-only mode. A series of lenses accelerated the ions and the final translational energy was 8250 eV. The fast ions entered a collision cell in which dimethyldisulfide was introduced as a neutralization gas to achieve 70% transmittance (T) of the precursor ion current. At this transmittance, >85% of the colliding ions underwent single collisions. The neutrals and ions exited the collision cell and entered the conduit region. The fast ions were deflected by the first element of the conduit, which was floated at +250 V, while the neutrals passed unhindered. The lifetime of the neutrals in the 60 cm long conduit was 3.2 μs . The surviving neutrals and fragments were then reionized in a second collision cell by O_2 introduced to achieve 70% T of the precursor ion current. The fast ions were decelerated to 80 eV translational energy, energy filtered, mass analyzed by a second quadrupole, and detected by an off-axis electron multiplier. The signal was converted to a voltage and amplified by a Keithley 428 amplifier. A series of scans, usually 30–50, were collected and processed by a PC based control system.

Variable time experiments were performed using the procedure described previously [38]. The lifetime of the neutrals and reionized fragments and survivor ions were varied in an inverse fashion by applying a scanning high voltage potential to various portions of the conduit. Using the ratio of integrated peak intensities for the survivor ion to fragment ion, fragment

mass, reionization efficiencies (the latter calculated using the method of Fitch and Sauter [39]) the dissociation rate constants for neutral and ionic dissociations could be calculated. A least squares fit was calculated for a bimodal exponential decay for one fast and one slow dissociation of the neutral intermediate, and for a single exponential decay of the reionized ion. A Visual Basic macro was used to integrate the kinetic equations for unimolecular dissociations for both neutrals and ions.

Collisionally activated dissociations (CAD) were performed in the first field-free region of a JEOL-HX100 double-focusing mass spectrometer using linked B/E scans. Air was used as the collision gas at 50% and 70% T of the precursor ion beam.

2.2. Calculations

Standard ab initio and density functional theory calculations were performed using the GAUSSIAN 94 suite of programs [40]. Geometries were optimized using Becke's hybrid functional (B3LYP) [41] and the 6-31 + G(d,p) basis set. For selected species and dissociation pathways, geometries were also optimized with MP2(FULL) and the 6-31 + G(d,p) basis set. Basis sets of this quality have been shown to give mostly reliable equilibrium geometries for neutral molecules and ions [42]. The optimized structures were characterized by harmonic frequency analysis as local minima (all frequencies real) or first-order saddle points (one imaginary frequency). The B3LYP/6-31 + G(d,p) frequencies were scaled by 0.961 [43] and used to calculate zero-point energies and enthalpy corrections. Single-point energies were calculated at the Gaussian-2(MP2) level of theory [44]. This consisted of MP2/6-311 + G(3df,2p), MP2/6-311G(d,p), and QCISD(T)/6-311G(d,p) [45] calculations that were combined to provide effective QCISD(T)/6-311 + G(3df,2p) energies corrected for the ZPVE and the number of valence electrons [44]. Note that most relative energies calculated in this work refer to isoelectronic systems in which the empirical corrections cancel out. In homolytic bond dissociations, treating the radical products by the G2(MP2) formalism formally violates spin conservation because un-

paired electrons are defined to have α spins. This causes the G2(MP2) homolytic bond dissociation energies to be $12.13 \text{ kJ mol}^{-1}$ greater than those calculated from effective QCISD(T)/6-311 + G(3df,2p) energies and appropriate ZPVE corrections. It should be noted that the G2(MP2) scheme was calibrated to atomization energies of mostly closed shell molecules to produce high atomic spin states, (^3P)O, (^3P)C, (^4S)N, etc. [44]. Hence, the empirical corrections using α electrons may somewhat underestimate the product stabilities and thus increase the homolytic bond dissociation energies. Franck–Condon energies in vertical neutralization and reionization were taken as absolute differences between the total energies of fully optimized ion or neutral structures and those in which an electron has been added to an optimized cation structure or subtracted from an optimized neutral structure. No zero-point corrections were applied to the calculated Franck–Condon energies.

3. Results and discussion

3.1. Ion preparation and characterization

Electron impact ionization of nitromethane as well as protonation with H_3^+ and CH_3^+ gave rise to $[\text{C},\text{H}_3,\text{N},\text{O}]^{++}$ ions at m/z 45 [Scheme 1, Eqs. (1) and (2)]. The highly exothermic protonation with H_3^+ provided the highest yield of $[\text{C},\text{H}_3,\text{N},\text{O}]^{++}$ as shown in Fig. 1. The CAD spectra of $[\text{C},\text{H}_3,\text{N},\text{O}]^{++}$ ions generated from nitromethane were practically identical; that from protonation with H_3^+ is shown in Fig. 2(a). The major dissociations of $[\text{C},\text{H}_3,\text{N},\text{O}]^{++}$ were loss of H^+ and CH_3 giving rise to fragment ions at m/z 44 and 30. The CAD spectrum in Fig. 2(a) was closely similar to that assigned to the nitrosomethane ion (2^{++}) by Hop et al. [33].

The 70 eV electron ionization mass spectrum of ethyl nitrite gave rise to a peak at m/z 45 that was found by high resolution measurements to consist of a 2.5:1 mixture of $[\text{C},\text{H}_3,\text{N},\text{O}]^{++}$ and $\text{C}_2\text{H}_5\text{O}^+$. The latter ion was not studied in detail, but it was assumed that it corresponded to the stable $\text{CH}_3\text{CH}=\text{OH}^+$ iso-

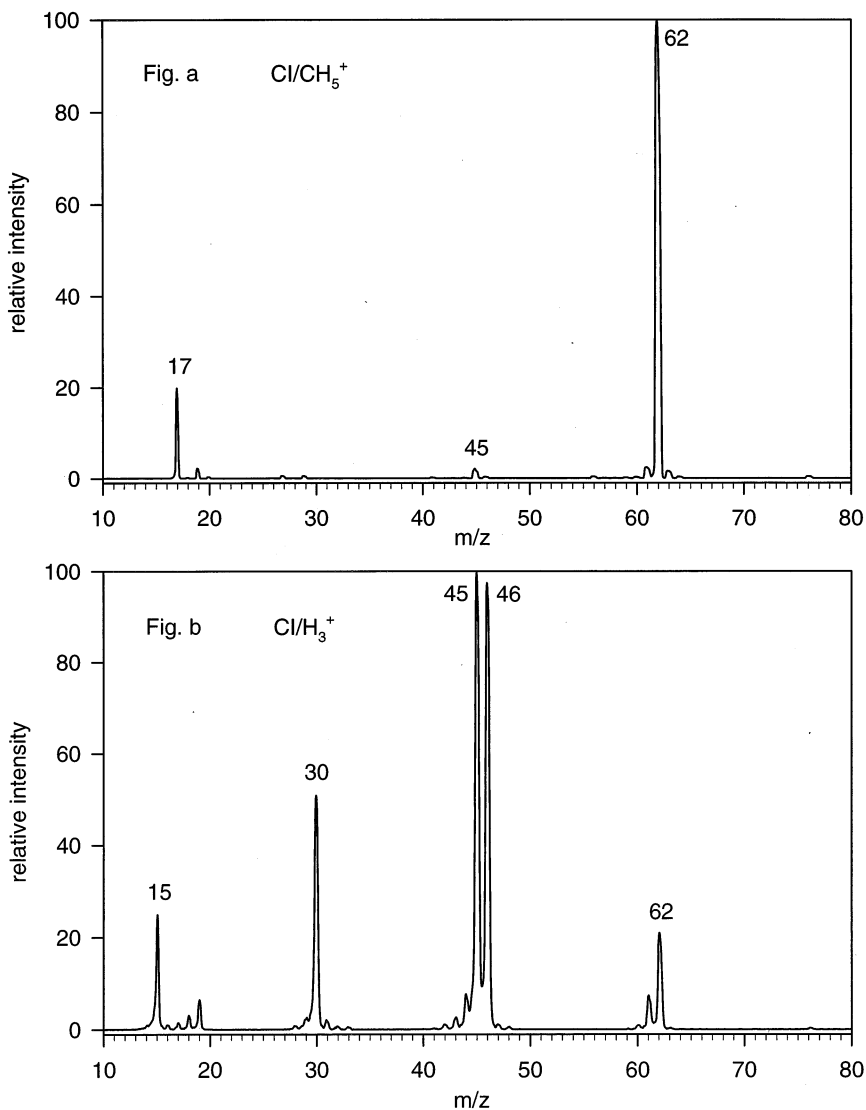


Fig. 1. Chemical ionization mass spectra of nitromethane. Protonation with (a) CH₅⁺, (b) H₃⁺.

mer, by analogy with the formation of CH₂=OH⁺ from methyl nitrite [6,7]. The [C,H₃,N,O]⁺ and C₂H₅O⁺ ions were separated in the mass spectra of labeled ethyl nitrite analogues, CH₃CD₂ONO and CD₃CD₂ONO. The mass spectrum of CH₃CD₂ONO gave a 5:1 mixture of [C,H₃,N,O]⁺ and C₂H₃DO⁺ at *m/z* 45, whereas the CH₃CD=OD⁺ ion appeared at *m/z* 47. The mass spectrum of CD₃CD₂ONO gave [C,D₃,N,O]⁺ at *m/z* 48, whereas CD₃CD=OD⁺ ap-

peared at *m/z* 50. The CAD spectra of [C,H₃,N,O]⁺ prepared from ethyl nitrite and CH₃CD₂ONO are shown in Fig. 2(b) and (c). In spite of some degree of contamination by the isobaric species, the CAD spectra of [C,H₃,N,O]⁺ closely resembled that of 2⁺.

The deuterium labeling measurements indicated that the expulsion of formaldehyde from the ethyl nitrite ion involved an intact CH₂-O moiety, which did not exchange hydrogen atoms with the methyl

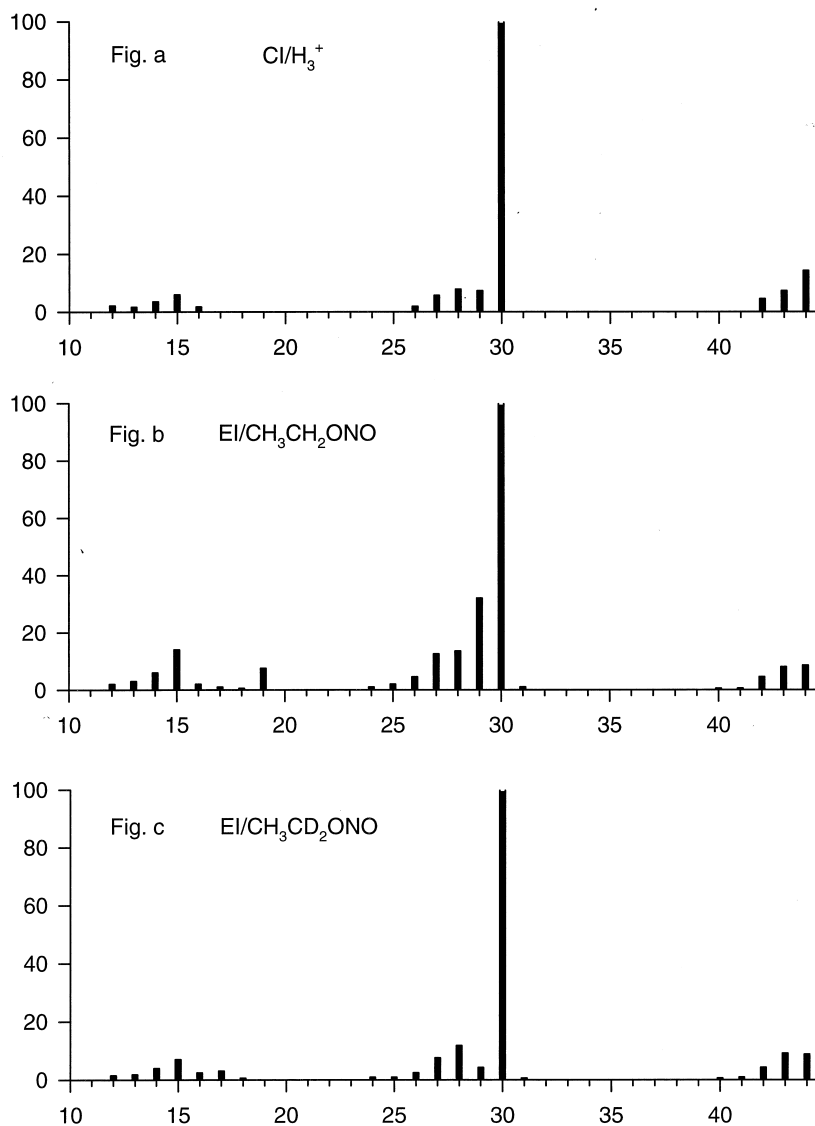
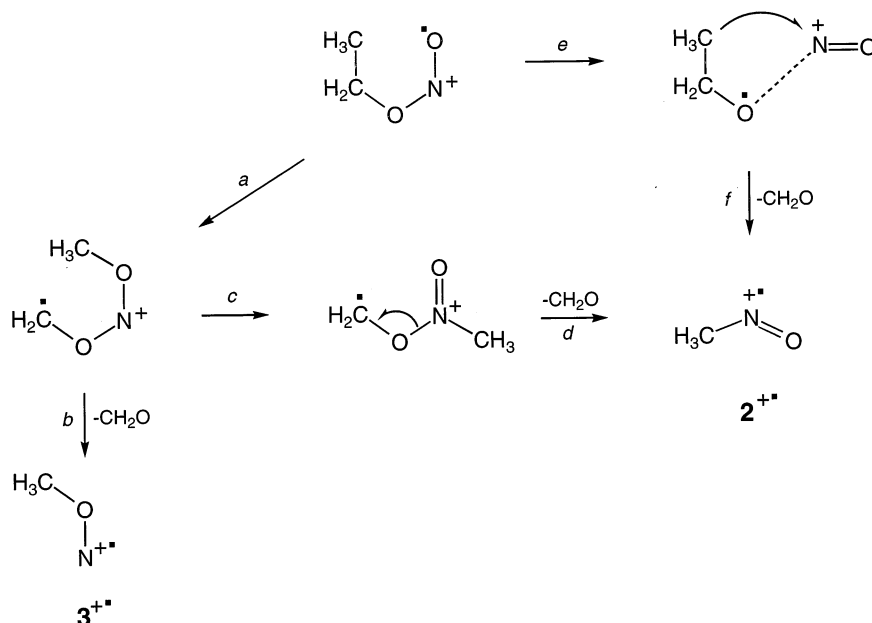


Fig. 2. CAD spectra of $[C,H_3,N,O]^{2+}$ prepared from various precursors: (a) 2^{++} from H_3^+ -protonated nitromethane; (b) 2^{++} from dissociation of ethyl nitrite ion; (c) 2^{++} from dissociation of $CH_3CD_2ONO^+$.

group. The methyl group can migrate to the N or O atoms of the NO moiety to give rise to 2^{++} or CH_3ON^{++} (3^{++}). These isomers can be expected to undergo similar dissociations, namely, loss of CH_3 to form NO^+ and may be difficult to distinguish. However, we show below that a clear distinction can be made on the basis of the calculated relative energies that strongly favor 2^{++} .

The mechanism for the elimination of formaldehyde from the ethyl nitrite ion is visualized in Scheme 2 that shows some of the alternative mechanisms for the methyl migration. Migration to the oxygen terminus may proceed through a five-membered transition state to form a distonic intermediate (path *a*), which can dissociate to form 3^{++} (path *b*) or rearrange by methyl migration to nitrogen (path *c*). A N–O bond



Scheme 2.

cleavage in the ethyl nitrite ion may lead to an ion–molecule complex of ethoxy radical and NO^+ (path *e*). Dissociation of the complex can proceed by loss of $\text{C}_2\text{H}_5\text{O}^\bullet$, which is the major path observed in the mass spectrum, or by methyl migration and elimination of formaldehyde to give $2^{+\bullet}$ (path *f*). Ion $2^{+\bullet}$ may also be formed by path *d*. In order to distinguish the $a \rightarrow b \rightarrow 3^{+\bullet}$ pathway in Scheme 2, it was necessary to unequivocally identify the ion formed and examine the product thermochemistry. This was achieved by a combination of NR mass spectra and ab initio calculations, as discussed below.

3.2. Neutral preparation and characterization

Collisional neutralization of $2^{+\bullet}$ followed by reionization afforded the NRMS spectrum shown in Fig. 3(a) and (b). The spectrum displayed a prominent survivor ion at m/z 45, and fragments at m/z 44, 30, 15, and 14. The NR mass spectra obtained from nitromethane protonated with H_3^+ and CH_5^+ were practically identical [Fig. 3(a) and (b)]. Overall, the NR mass spectra in Fig. 3 were very similar to that assigned to $2^{+\bullet}$ by Hop et al. [33]. Note that the latter

authors used xenon as neutralization gas and obtained the spectra on a sector instrument. The NR mass spectra of $[\text{C}_2\text{H}_3\text{N}_2\text{O}]^{+\bullet}$ from ethyl nitrite and $\text{CH}_3\text{CD}_2\text{ONO}$ showed dissociations characteristic of $2^{+\bullet}$ when accounting for the contaminating ions [Fig. 4(a)–(c)]. Subtracting a reference NR mass spectrum of $\text{CH}_3\text{CH}=\text{OH}^+$ (prepared from 2-propanol) from the spectrum in Fig. 4(a) resulted in a spectrum that was closely similar to that of $2^{+\bullet}$ from nitromethane. The NR spectrum of $\text{CD}_3\text{NO}^{+\bullet}$ from $\text{CD}_3\text{CD}_2\text{ONO}$ showed a somewhat more abundant $(\text{M} - \text{D})^+$ peak at m/z 46 [Fig. 4(c)], but otherwise was similar to that of $2^{+\bullet}$. The peak at m/z 28 in the NR mass spectra of both $2^{+\bullet}$ and $\text{CD}_3\text{NO}^{+\bullet}$ was assigned to $\text{CO}^{+\bullet}$.

In order to distinguish dissociations of neutral **2** from those of reionized $2^{+\bullet}$ we performed variable-time measurements for the most abundant channel forming CH_3 and NO . Ions $2^{+\bullet}$ used in these measurements were generated by CD_2O elimination from $\text{CH}_3\text{CD}_2\text{ONO}^{+\bullet}$ [Fig. 4(b)]. The rate parameters for dissociations of neutral **2** were measured as $k_{\text{N}}(\text{NO}) = (8.2 \pm 0.8) \times 10^5 \text{ s}^{-1}$ and $k_{\text{N}}(\text{CH}_3) = (5.6 \pm 0.6) \times 10^5 \text{ s}^{-1}$. The rate parameters showed a reasonable albeit not perfect correlation. The rate

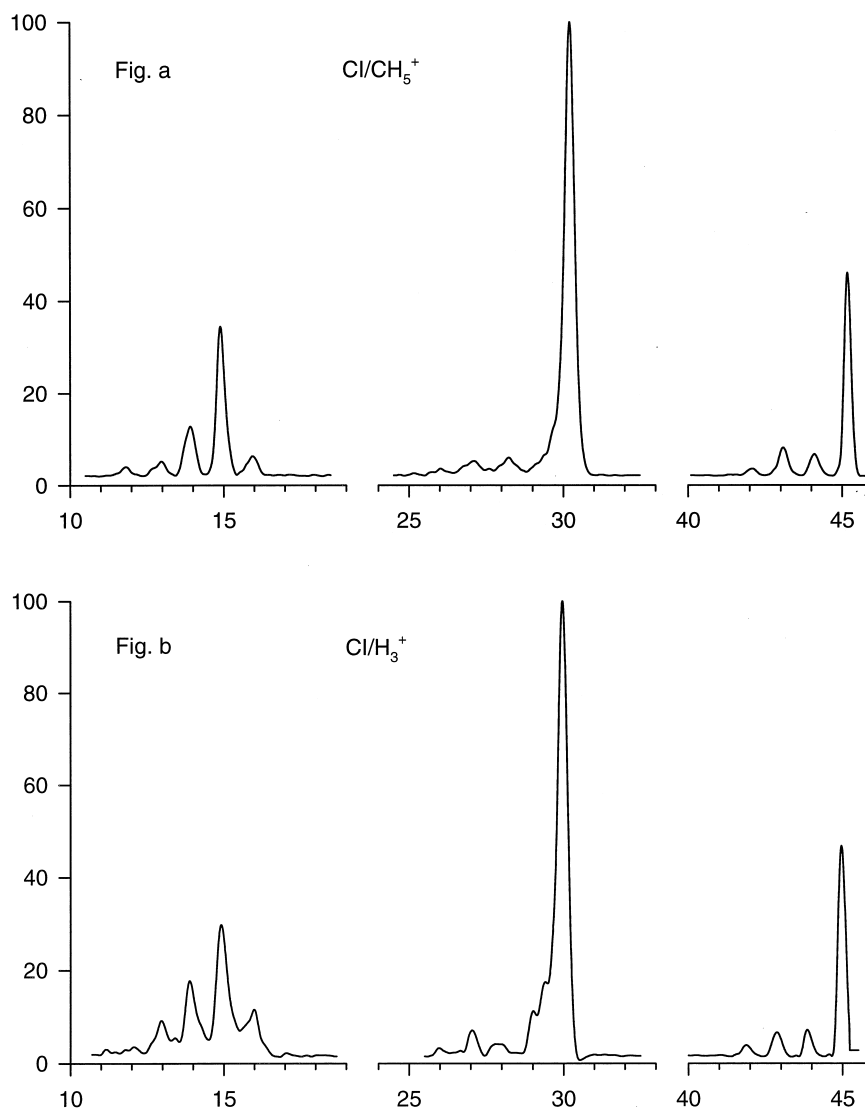


Fig. 3. Neutralization (CH_3SSCH_3 , 70% T) reionization (O_2 , 70% T) mass spectra of (a) 2^{++} from CH_5^+ -protonated nitromethane; (b) 2^{++} from H_3^+ -protonated nitromethane.

parameters for the dissociations of reionized 2^{++} , $k_i(\text{NO}^+) = (6.1 \pm 1.6) \times 10^5 \text{ s}^{-1}$ and $k_i(\text{CH}_3^+) = (-5.1 \pm 8) \times 10^4 \text{ s}^{-1}$, showed preferential formation of NO^+ in line with the ordering of ionization energies, $\text{IE}(\text{NO}) = 9.264 \text{ eV} < \text{IE}(\text{CH}_3) = 9.84 \text{ eV}$ [46]. The variable-time measurements clearly showed that *both* neutral and ion dissociations occurred on NR. The N–O bond dissociation energies in **2** and 2^{++}

were therefore investigated by ab initio and density functional calculations, as discussed below.

3.3. Ion structures and energies

The B3LYP/6-31 + G(d,p) optimized ion structures are shown in Fig. 5. Two features deserve a brief comment. The C–O bond in the isonitrosomethane ion

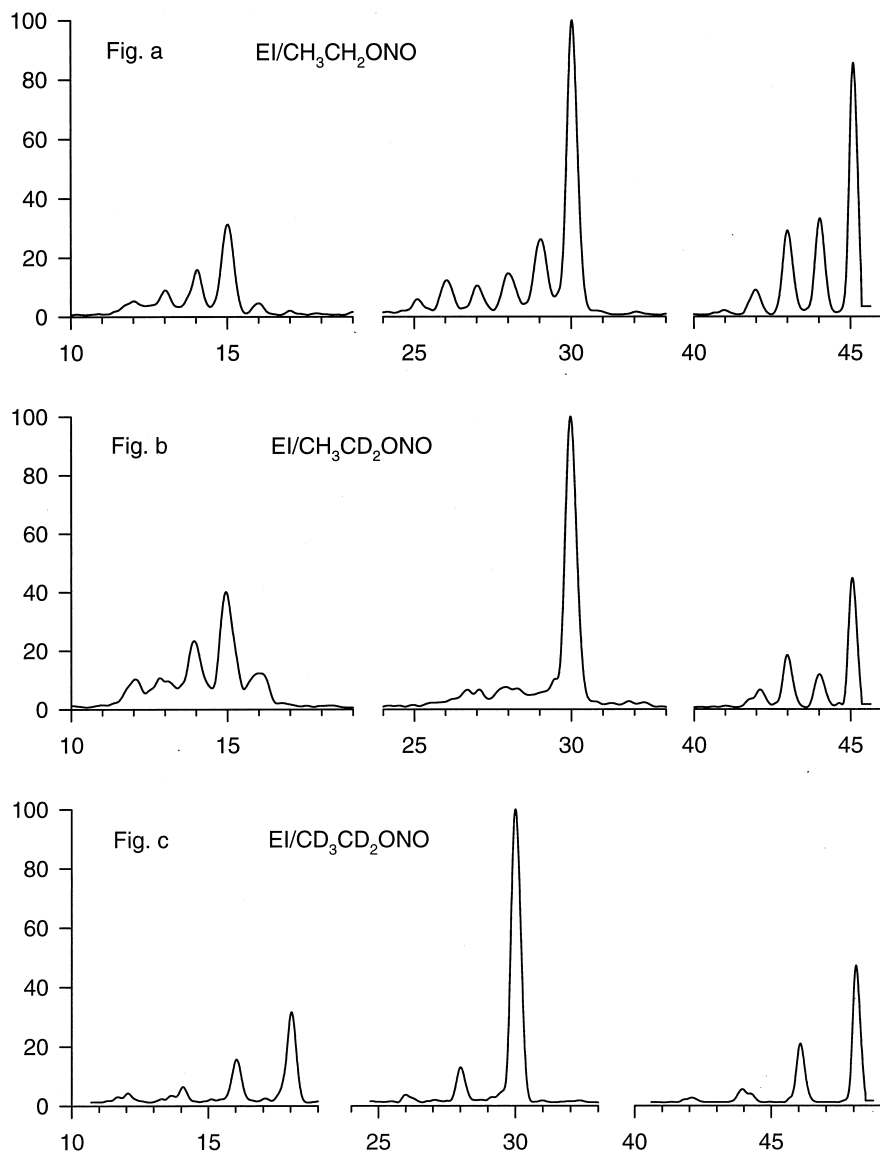


Fig. 4. Neutralization (CH_3SSCH_3 , 70% *T*) reionization (O_2 , 70% *T*) mass spectra of (a) $2^{++} + \text{CH}_3\text{CH}=\text{OH}^+$ from ethyl nitrite; (b) 2^{++} from $\text{CH}_3\text{CD}_2\text{ONO}$; (c) $[2\text{-D}_3]^{++}$ from $\text{CD}_3\text{CD}_2\text{ONO}$.

(3^{++}) is conspicuously long and the H–C–O angles are small indicating partial planarization of the methyl group. Ion 3^{++} may be viewed as a complex of a methyl radical bound to the oxygen terminus of the NO^+ cation. Note that no dramatic lengthening of the C–N bond was calculated for 2^{++} (Fig. 5). The formaldoxime ion 4^{++} was found to exist as a single,

gauche rotamer in which both the O–H and the C–H bonds were deflected out of the C–N–O plane. Two planar structures corresponding to syn and antirotamers were calculated to be transition states for OH group rotation in 4^{++} . The rotational barriers, calculated with B3LYP/6-31 + G(d,p), were substantial, 85 and 29 kJ mol^{-1} for the syn and anti-transition

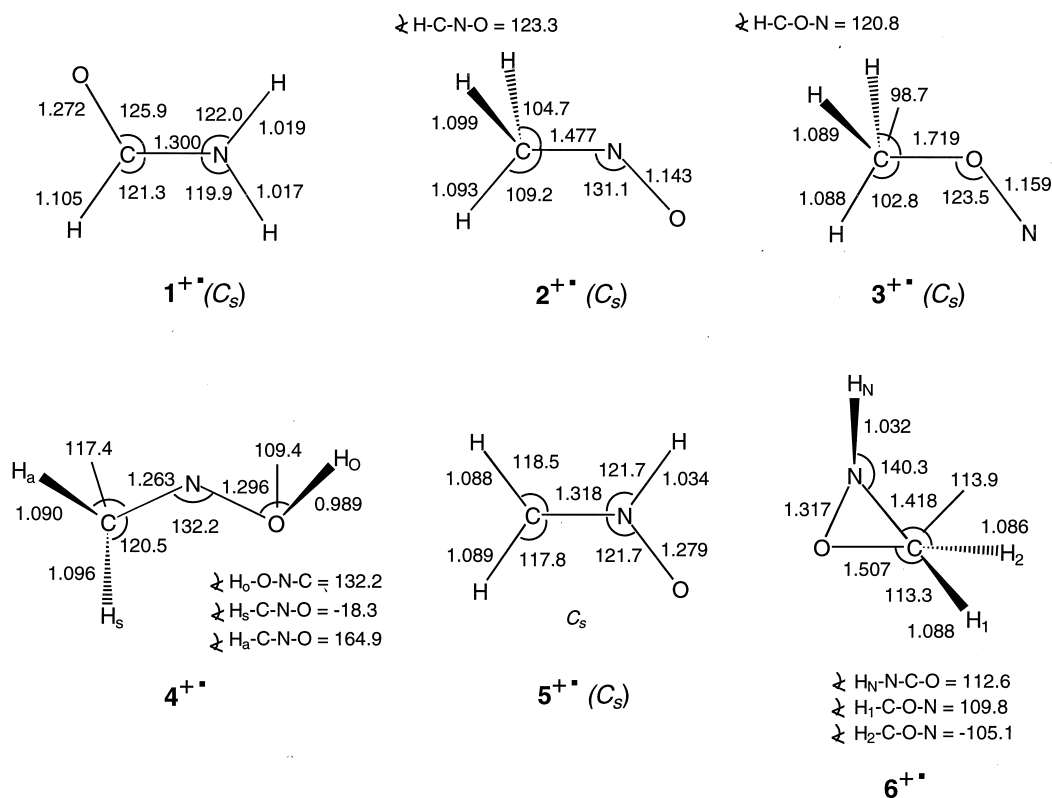


Fig. 5. B3LYP/6-31 + G(d,p) optimized geometries of 1^{+*} – 6^{+*} . Bond lengths in angstroms, bond and dihedral angles in degrees.

states, respectively. This contrasted the optimized geometries of neutral **4** that showed two stable planar rotamers (vide infra).

The ion relative energies are summarized in Table 1. According to G2(MP2), ions 2^{+*} – 6^{+*} were 160–250 kJ mol^{-1} less stable than 1^{+*} confirming that they belonged to a group of high-energy isomers. The relative energies obtained with B3LYP/6-311 + G(3df,2p) showed the same ordering of isomer stabilities, although absolute deviations of up to 16 kJ mol^{-1} were apparent (Table 1). In addition to the relative stabilities of the high-energy ion isomers 2^{+*} – 6^{+*} , dissociation energies due to simple bond cleavages were calculated at the corresponding thermochemical thresholds, that is, disregarding potential energy barriers (Table 2).

The lowest-energy dissociation of 2^{+*} was formation of CH_3 and NO^+ . The formation of charge-reversed products, CH_3^+ and NO , and loss of H to

form $\text{CH}_2=\text{N}=\text{O}^+$ required higher threshold energies. The calculated threshold energies were in good qualitative agreement with the product ion formations in the CAD spectrum of 2^{+*} , which showed a dominant NO^+ ion [Fig. 2(a)]. The CAD relative intensities of the minor ions, CH_3^+ and $\text{CH}_2=\text{N}=\text{O}^+$, which did not follow the order of threshold dissociation energies, may be biased by different ion transmission and detection efficiencies at different ion kinetic energies and m/z values.

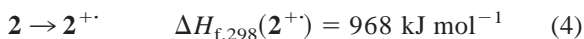
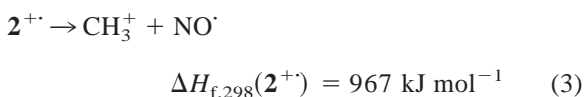
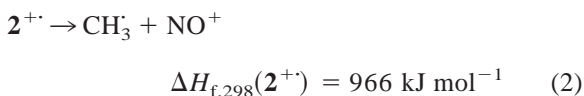
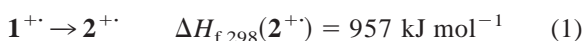
The thermochemistry of 2^{+*} and the other high-energy $[\text{C},\text{H}_3,\text{N},\text{O}]^{+*}$ isomers can be assessed from the ion relative and dissociation energies and adiabatic ionization energies of the neutral molecules (Table 3, vide infra). The relative energy scale was anchored to the experimental heat of formation of 1^{+*} ($\Delta H_{f,298}^{\circ} = 794 \text{ kJ mol}^{-1}$), which was obtained using the tabulated $\Delta H_{f,298}^{\circ}(\mathbf{1}) = -186 \text{ kJ mol}^{-1}$ and $\text{IE}_a(\mathbf{1}) = 10.16 \text{ eV}$ [46]. This reference number

Table 1
Relative energies of $[\text{C}_2\text{H}_3\text{N}_2\text{O}]^{2+}$ ions and molecules (kJ mol^{-1})

Species	B3LYP/6-311 + G(3df,2p)		QCISD(T)/6-311 + G(3df,2p)	
	0 K	298 K	0 K	298 K
Ions				
1²⁺	0	0	0	0
2²⁺	176	177	161	163
3²⁺	266	269	253	256
			(250) ^a	
4²⁺	187	187	190	190
5²⁺	182	182	183	183
6²⁺	264	264	248	248
Neutrals				
1	0	0	0	0
2	268	268	257	257
3	464	464	459	459
anti- 4	215	215	208	208
syn- 4	235	234	229	228
5	254	253	254	253
6	308	307	291	289

^a Single-point calculations on a MP2(FULL)/6-31 + G(d,p) optimized geometry using B3LYP/6-31 + G(d,p) zero-point corrections.

slightly differed from that used by Hop et al. (791 kJ mol^{-1}) [33]. The calculated $\Delta H_{f,298}(\mathbf{2}^{2+})$ are shown in Eqs. (1)–(4)



The estimate from the ion relative energies [Eq. (1)] is somewhat lower than those from ion dissociations [Eqs. (2) and (3)] and neutral ionization [Eq. (4)]. The heats of formation from Eqs. (2)–(4) very nicely confirm the previous estimate by Hop et al. (967 kJ mol^{-1} [33]).

Equations analogous to (1)–(4) were also used to calculate $\Delta H_{f,298}(\mathbf{3}^{2+})$, as 1050, 1065, 1067, and 1054 kJ mol^{-1} , respectively. The average value, $1059 \pm 8 \text{ kJ mol}^{-1}$, represents the best estimate for the high-energy isomer $\mathbf{3}^{2+}$. It may be noted (Table 2) that ion $\mathbf{3}^{2+}$ is only weakly bound against dissociation to CH_3 and NO^+ .

The thermochemistry of ions $\mathbf{4}^{2+}$ – $\mathbf{6}^{2+}$ was assessed from the relative ion energies and adiabatic ionization energies (Table 3). The latter were combined with G2(MP2) calculated heats of formation of the neutral molecules (vide infra). The $\Delta H_{f,298}$ calculated from the relative energies and ionization energies agreed within 10 kJ mol^{-1} giving the following averaged values: $\Delta H_{f,298}(\mathbf{4}^{2+}) = 989 \pm 5 \text{ kJ mol}^{-1}$, $\Delta H_{f,298}(\mathbf{5}^{2+}) = 982 \pm 5 \text{ kJ mol}^{-1}$, $\Delta H_{f,298}(\mathbf{6}^{2+}) = 1046 \pm 5 \text{ kJ mol}^{-1}$. It should be noted that the use of the empirical (“high level”) corrections in the G2(MP2) energies [44] sometimes results in ionization energies that are ~ 0.1 – 0.15 eV too high [47]. For example, the IE_a of **1** (10.16 eV) [46] was calculated with a better accuracy without using the “high level” correction (10.13 eV) than with it (10.26 eV , Table 3).

It was interesting to compare the performance of the density functional theory method used (B3LYP) in providing accurate dissociation and ionization energies for the ions in question. Table 2 shows that the B3LYP/6-311 + G(3df,2p) calculations uniformly *overestimated* ion dissociation energies by as much as 40 kJ mol^{-1} . This appears to be typical for dissociations of open-shell species [48,49], and it was attributed to the possibility that a better delocalization of

Table 2
Dissociation energies (kJ mol⁻¹)

Reaction	B3LYP/6-311 + G(3df,2p)		QCISD(T)/6-311 + G(3df,2p)		Exp.
	0 K	298 K	0 K	298 K	
2 → CH ₃ + NO [•]	147	153	154	161	163 ^a
2 → TS(CH ₃ . . . NO)			148		
3 → CH ₃ + NO [•]	-49	-42	-48	-41	
3 → TS(CH ₃ . . . ON)			-9		
anti- 4 → CH ₂ =N-O [•] + H [•]	322	327	340	346	
5 → CH ₂ =N-O [•] + H [•]	283	289	295	301	
2 ⁺ → CH ₃ ⁺ + NO ⁺	199	205	157	164	166 ^b
2 ⁺ → CH ₃ ⁺ + NO [•]	222	228	211	218	218 ^b
2 ⁺ → CH ₂ =N=O ⁺ + H [•]	261	266	253	258	
3 ⁺ → CH ₃ ⁺ + NO ⁺	109	105	68	65	
4 ⁺ → HC=N-OH ⁺ + H [•]	218	225	189	196	
4 ⁺ → CH ₂ =N=O ⁺ + H [•]	250	256	224	230	
5 ⁺ → CH ₂ =N=O ⁺ + H [•]	255	261	231	238	

^a From [50].

^b From the reactant and product heats of formation [46].

valence electrons in an open-shell reactant, which is described by a larger wavefunction than the open shell product, is amplified by the density functional treat-

ment and results in an overstabilization of the larger species. In contrast, ionization and recombination energies were reproduced rather well by B3LYP when

Table 3
Ionization and recombination energies in the [C,H₃,N,O] system

Species		B3LYP	QCISD(T)	G2(MP2)	Exp. ^a
		6-311 + G(3df,2p)			
Formamide (1)	IE _a ^b	10.13	10.13	10.26	10.16
	IE _v ^c	10.33	10.35	10.48	10.16
	RE _v ^d	9.87			
CH ₃ NO (2)	IE _a	9.17	9.14	9.27	9.3
	IE _v	9.67	9.60	9.73	9.68
	RE _v	8.61	8.51	8.63	
CH ₃ ON (3)	IE _a	8.07	7.97	8.10	
	IE _v	8.42			
	RE _v	7.93			
CH ₂ =NOH (4)	IE _a	9.83	9.94	10.07	10.11
	IE _v	10.92	10.99	11.10	10.60
	RE _v	8.84	8.88	8.99	
CH ₂ =NH-O (5)	IE _a	9.38	9.40	9.53	
	IE _v	9.46	9.42	9.53	
	RE _v	9.30	9.35	9.46	
cyc-CH ₂ -NH-O (6)	IE _a	9.67	9.69	9.82	
	IE _v	10.61	10.65	10.76	
	RE _v	8.55	8.48	8.59	

^a Adiabatic ionization energies were extrapolated from onsets in photoelectron spectra [24].

^b Adiabatic ionization energy, eV.

^c Vertical ionization energy, eV.

^d Vertical recombination energy, eV.

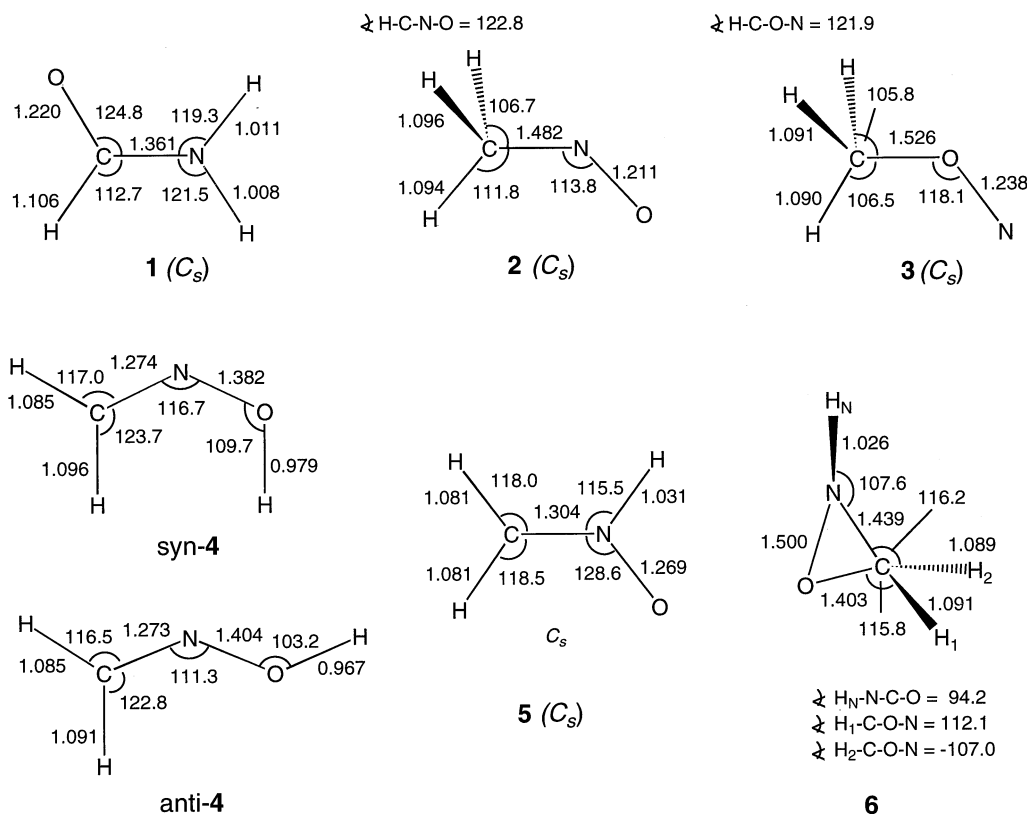


Fig. 6. B3LYP/6-31 + G(d,p) optimized structures of 1–6.

compared with the G2(MP2) and experimental data (Table 3). The largest deviation in the calculated IE was found for **4** where the B3LYP values were off by 0.2–0.3 eV.

3.4. Neutral structures and energies

The optimized structures of **1–6** are depicted in Fig. 6. The structures of **2**, **4**, and **5**, calculated at various levels of theory, were discussed in detail previously [27–31] and compared with available experimental geometries from microwave spectra [25,26]. The B3LYP/6-31 + G(d,p) optimized geometries of **2** and **4** showed bond lengths and angles that were in excellent agreement with the experimental data [25,26]. The thermochemistry of **2** was assessed from the atomization energy [Eq. (5)], an isodesmic

reaction [Eq. (6)], dissociation [Eq. (7)], and energy relative to that of **1** [Eq. (8)]



$$\Delta H_{\text{f},298}^{\circ}(\mathbf{2}) = 62 \text{ kJ mol}^{-1} \quad (5)$$



$$\Delta H_{\text{f},298}^{\circ}(\mathbf{2}) = 71 \text{ kJ mol}^{-1} \quad (6)$$



$$\Delta H_{\text{f},298}^{\circ}(\mathbf{2}) = 75 \text{ kJ mol}^{-1} \quad (7)$$



$$\Delta H_{\text{f},298}^{\circ}(\mathbf{2}) = 71 \text{ kJ mol}^{-1} \quad (8)$$

The $\Delta H_{f,298}^{\circ}$ from Eq. (5) appeared to be somewhat low. This was checked by calculating the $\Delta H_{f,298}^{\circ}$ of **1** based on its atomization energy, which again gave a low value, -195 kJ mol^{-1} compared with the experimental -186 kJ mol^{-1} [46]. Eq. (5) was therefore excluded from the thermochemical calculations. The mean value of Eqs. (6)–(8), $\Delta H_{f,298}^{\circ}(\mathbf{2}) = 72 \pm 2 \text{ kJ mol}^{-1}$, was in excellent agreement with an estimate from the C–N bond dissociation energy [50] ($73 \pm 6 \text{ kJ mol}^{-1}$). The $\Delta H_{f,298}^{\circ}$ of the other isomers was assessed from the relative energies referenced to **1** as $\Delta H_{f,298}^{\circ}(\mathbf{3}) = 273 \text{ kJ mol}^{-1}$, $\Delta H_{f,298}^{\circ}(\mathbf{4}) = 22 \text{ kJ mol}^{-1}$, $\Delta H_{f,298}^{\circ}(\mathbf{5}) = 67 \text{ kJ mol}^{-1}$, and $\Delta H_{f,298}^{\circ}(\mathbf{6}) = 103 \text{ kJ mol}^{-1}$.

The dissociation energy of the C–N bond in neutral **2** was comparable to that in ion $\mathbf{2}^{+}$ (Table 2). The calculated bond dissociation energy in **2** was in excellent agreement with the single experimental value (163 kJ mol^{-1}) [50]. We have also examined the potential energy surface along the dissociation pathway to determine if there is a barrier corresponding to a transition state. Stepwise calculations with B3LYP/6-31 + G(d,p) showed a very shallow rise of potential energy (e.g. 12 kJ mol^{-1} at $d(\text{C–N}) = 2.7 \text{ \AA}$) in spite of the substantial bond dissociation energy predicted at this level of theory (151 kJ mol^{-1}). It appeared that B3LYP was not treating the $\text{CH}_3 \dots \text{NO}$ system properly, and the dissociation pathway was therefore reexamined with MP2(FULL)/6-31 + G(d,p) calculations, which yielded a first-order saddle point at $d(\text{C–N}) = 3.2 \text{ \AA}$. However, a single-point G2(MP2) calculation placed the putative transition state 6 kJ mol^{-1} below the dissociation threshold. It therefore appeared that the C–N bond dissociation in **2** was continuously endothermic. The similarity of the BDE in **2** and $\mathbf{2}^{+}$ is consistent with the similar rate parameters for the neutral and ion dissociations (vide supra). It is also of interest to note that the dissociation threshold for CH_3 and NO^{\cdot} was substantially below the barrier to unimolecular isomerization of **2** to the more stable syn-**4**. The latter barrier was estimated at $254\text{--}263 \text{ kJ mol}^{-1}$ from recent MP2 and B3LYP calculations [27].

A transition state was also sought for the exothermic dissociation of **3** to CH_3 and NO^{\cdot} . MP2(FULL)/

6-31 + G(d,p) calculations located a first-order saddle point at $d(\text{C–O}) = 1.905 \text{ \AA}$. However, a G2(MP2) single point calculation placed the putative transition state 9 kJ mol^{-1} below the energy of **3**. This indicated that higher level calculations, in both optimizations and single points, would be needed to treat the dissociation of **3** accurately. Nonetheless, the calculations strongly indicated that **3** was a very weakly bound species that should not have a microsecond lifetime when formed by collisional neutralization. Note also (Table 3) that the Franck–Condon energy in vertical neutralization of $\mathbf{3}^{+}$ should be sufficient to cause rapid dissociation of **3**.

As a final note, the N–H bond dissociation energy in nitron **5** was substantial, 301 kJ mol^{-1} at 298 K (Table 3). This, together with the high potential energy barrier to isomerization to anti-**4** ($185\text{--}200 \text{ kJ mol}^{-1}$ [27]), should make **5** amenable to preparation in the gas phase.

4. Conclusions

Nitrosomethane cation radical $\mathbf{2}^{+}$ is formed by loss of an O atom from the nitromethane cation radical and by loss of OH^{\cdot} from protonated nitromethane. The newly discovered elimination of formaldehyde from the ethyl nitrite cation radical also gives rise to ion $\mathbf{2}^{+}$ and not the isonitrosomethane ion $\mathbf{3}^{+}$. A combination of ion and neutral thermochemistry from high-level ab initio calculations, and ion characterization by NRMS allowed us to distinguish among several alternative mechanisms of ethyl nitrite ion dissociation.

Acknowledgements

Support of this work by the National Science Foundation (Grants CHE-9712750 and CHE-9808182) is gratefully acknowledged.

References

- [1] (a) H. Egsgaard, L. Carlsen, in *The Chemistry of Amino, Nitroso, Nitro and Related Groups*, S. Patai (Ed.), Wiley,

- Chichester, 1996, Supplement F2, Part 1. (b) H. Schwarz, K. Levsen, in *The Chemistry of Amino, Nitroso, Nitro and Related Groups*, S. Patai (Ed.), Wiley, Chichester, 1982, Supplement E, Part 1.
- [2] (a) G.G. Meisels, T. Hsieh, J. Gilman, *J. Chem. Phys.* 73 (1980) 1174, 4126. (b) J. Gilman, T. Hsieh, G.G. Meisels, *J. Chem. Phys.* 78 (1983) 3767.
- [3] H. Egsgaard, L. Carlsen, S. Elbel, *Ber. Bunsenges. Phys. Chem.* 90 (1986) 369.
- [4] N.M.M. Nibbering, Th.J. de Boer, H.J. Hofman, *Recl. Trav. Chim. Pays-Bas.* 84 (1965) 481.
- [5] S.K. Hindawi, R.H. Fokkens, F.A. Pinkse, N.M.M. Nibbering, *Org. Mass Spectrom.* 21 (1986) 243.
- [6] M. Sirois, J.L. Holmes, C.E.C.A. Hop, *Org. Mass Spectrom.* 25 (1990) 167.
- [7] D. Schroder, D. Sultze, O. Dutuit, T. Baer, H. Schwarz, *J. Am. Chem. Soc.* 116 (1994) 6395.
- [8] H. Egsgaard, L. Carlsen, *Chem. Phys. Lett.* 147 (1988) 30.
- [9] M.P. Irion, A. Selinger, A.W. Castleman Jr., E.E. Ferguson, K.G. Weil, *Chem. Phys. Lett.* 147 (1988) 33.
- [10] T. Baer, J.R. Hass, *J. Phys. Chem.* 90 (1986) 451.
- [11] D.V. Ramana, N.V.S. Rama Krishna, *Org. Mass Spectrom.* 24 (1989) 66.
- [12] D.V. Ramana, K.K. Balasubramanian, M.S. Sudha, T. Balasubramanian, *J. Am. Soc. Mass Spectrom.* 6 (1995) 195.
- [13] T. Nishimura, P.R. Das, G.G. Meisels, *J. Chem. Phys.* 84 (1986) 6190.
- [14] M.L. McKee, *J. Phys. Chem.* 90 (1986) 2335.
- [15] B. Leyh-Nihant, J.-C. Lorquet, *J. Chem. Phys.* 88 (1988) 5606.
- [16] C. Lifshitz, M. Rejwan, I. Levin, T. Peres, *Int. J. Mass Spectrom. Ion Processes* 84 (1988) 271.
- [17] P.C. Burgers, J.K. Terlouw, in *Mass Spectrometry: A Specialist Periodical Report*, M.E. Rose (Senior Reporter), Royal Society of Chemistry, Cambridge, 1989, Vol. 10, p. 67.
- [18] M. Polasek, F. Turecek, *J. Phys. Chem. A*, in press.
- [19] C.L. Coe, T.F. Doumani, *J. Am. Chem. Soc.* 70 (1948) 1516.
- [20] H.A. Taylor, H. Bender, *J. Chem. Phys.* 9 (1941) 761.
- [21] B.G. Gowenlock, J. Trotman, *J. Chem. Soc.* (1955) 4190.
- [22] E. Bamberger, R. Seligman, *Chem. Ber.* 36 (1903) 685.
- [23] P.D. Adeney, W.J. Bouma, L. Radom, W.R. Rodwell, *J. Am. Chem. Soc.* 102 (1980) 4049.
- [24] D.C. Frost, W.M. Lau, C.A. McDowell, N.P.C. Westwood, *J. Phys. Chem.* 86 (1982) 3577.
- [25] P.H. Turner, A.P. Cox, *J. Chem. Soc. Faraday Trans. II* 74 (1978) 533.
- [26] I.N. Levine, *J. Mol. Spectrosc.* 8 (1962) 276.
- [27] T. Vladimiroff, *THEOCHEM* 401 (1997) 141.
- [28] A.C. Samuels, J.O. Jensen, P.N. Krishnan, L.A. Burke, *THEOCHEM* 427 (1998) 199.
- [29] T.H. Thuemmel, *J. Phys. Chem. A* 102 (1998) 2002.
- [30] H. Basch, *Inorg. Chim. Acta* 252 (1996) 265.
- [31] I. Komaromi, J.M. Tronchet, *THEOCHEM* 366 (1996) 147.
- [32] H. Basch, P. Aped, S. Hoz, *Mol. Phys.* 89 (1996) 331.
- [33] C.E.C.A. Hop, H. Chen, P.J.A. Ruttink, J.L. Holmes, *Org. Mass Spectrom.* 26 (1991) 679.
- [34] For reviews see: (a) C. Wesdemiotis, F.W. McLafferty, *Chem. Rev.* 87 (1987) 485; (b) J.K. Terlouw, H. Schwarz, *Angew. Chem. Int. Ed. Engl.* 26 (1987) 805; (c) J.L. Holmes, *Mass Spectrom. Rev.* 8 (1989) 513; (d) J.K. Terlouw, *Adv. Mass Spectrom.* 11 (1989) 984; (e) F.W. McLafferty, *Science* 247 (1990) 925; (f) F. Turecek, *Org. Mass Spectrom.* 27 (1992) 1087; (g) N. Goldberg, H. Schwarz, *Acc. Chem. Res.* 27 (1994) 347; (h) C.A. Schalley, G. Hornung, D. Schroder, H. Schwarz, *Chem. Soc. Rev.* 27 (1998) 91.
- [35] D.W. Kuhns, T.B. Tran, S.A. Shaffer, F. Turecek, *J. Phys. Chem.* 98 (1994) 4845.
- [36] D.W. Kuhns, F. Turecek, *Org. Mass Spectrom.* 29 (1994) 463.
- [37] F. Turecek, M. Gu, S.A. Shaffer, *J. Am. Soc. Mass Spectrom.* 3 (1992) 493.
- [38] A.J. Frank, M. Sadilek, J.G. Ferrier, F. Turecek, *J. Am. Chem. Soc.* 119 (1997) 12 343.
- [39] W.L. Fitch, A.D. Sauter, *Anal. Chem.* 55 (1983) 832.
- [40] M.J. Frisch, G.W. Trucks, H.B. Schlegel, P.M.W. Gill, B.G. Johnson, M.A. Robb, J.R. Cheeseman, T.A. Keith, G.A. Petersson, J.A. Montgomery, K. Raghavachari, M.A. Al-Laham, V.G. Zakrzewski, J.V. Ortiz, J.B. Foresman, J. Ci-oslowski, B.B. Stefanov, A. Nanayakkara, M. Challacombe, C.Y. Peng, P.Y. Ayala, W. Chen, M.W. Wong, J.L. Andres, E.S. Replogle, R. Gomperts, R.L. Martin, D.J. Fox, J.S. Binkley, D.J. Defrees, J. Baker, J.P. Stewart, M. Head-Gordon, C. Gonzalez, J.A. Pople, *GAUSSIAN 94* (Revision D.1), Gaussian, Inc., Pittsburgh, PA, 1995.
- [41] (a) A.D. Becke, *J. Chem. Phys.* 98 (1993) 1372, 5648; (b) P.J. Stephens, F.J. Devlin, C.F. Chablowski, M.J. Frisch, *J. Phys. Chem.* 98 (1994) 11 623.
- [42] See for example: (a) C.W. Bauschlicher, H. Partridge, *J. Chem. Phys.* 103 (1995) 1788; (b) A.J. Frank, M. Sadilek, J.G. Ferrier, F. Turecek, *J. Am. Chem. Soc.* 118 (1996) 11 321; (c) F. Turecek, *J. Phys. Chem. A* 102 (1998) 4703.
- [43] (a) G. Rauhut, R. Pulay, *J. Phys. Chem.* 99 (1995) 3093; (b) J.W. Finley, P.J. Stephens, *J. Mol. Struct.: THEOCHEM* 357 (1995) 225; (c) M.W. Wong, *Chem. Phys. Lett.* 256 (1996) 391; (d) A.P. Scott, L. Radom, *J. Phys. Chem.* 100 (1996) 16 502.
- [44] (a) L.A. Curtiss, K. Raghavachari, J.A. Pople, *J. Chem. Phys.* 98 (1993) 1293; (b) L.A. Curtiss, K. Raghavachari, P.C. Redfern, J.A. Pople, *J. Chem. Phys.* 106 (1997) 1063; (c) K. Raghavachari, B.B. Stefanov, L.A. Curtiss, *J. Chem. Phys.* 106 (1997) 6764.
- [45] J.A. Pople, M. Head-Gordon, K. Raghavachari, *J. Chem. Phys.* 87 (1987) 5968.
- [46] W.G. Mallard, P.J. Linstrom (Eds.), *NIST Chemistry Webbook*, NIST Standard Reference Database, No. 69, National Institute of Standards and Technology, Gaithersburg, MD, 1998, <http://webbook.nist.gov/chemistry>
- [47] V.Q. Nguyen, F. Turecek, *J. Mass Spectrom.* 31 (1996) 843.
- [48] F. Turecek, *J. Mass Spectrom.* 33 (1998) 779.
- [49] F. Turecek, J.K. Wolken, *J. Phys. Chem. A* 103 (1999) 1905.
- [50] L. Batt, R.T. Milne, *Int. J. Chem. Kinet.* 5 (1973) 1067.